1996

The generation of quasi-inertial oscillations during upwelling off the southern coast of the Crimea

Vlasenko, Vasyl

http://hdl.handle.net/10026.1/3839

Oceanology

Oceanology, Vol. 36, No. 1, 1996, pp. 38–45. Translated from Okeanologiya, Vol. 36, No. 1, 1996, pp. 43–51.

MARINE PHYSICS

The Generation of Quasi-Inertial Oscillations during Upwelling off the Southern Coast of Crimea

V. I. Vlasenko, V. A. Ivanov, and N. M. Stashchuk

Marine Hydrophysical Institute, National Academy of Sciences of Ukraine, Sevastopol, Ukraine

Received April 14, 1994

Abstract—The response of the Black Sea shelf zone to the effect of short-term (less than one day) winds is studied. Mathematical modeling is carried out numerically on the basis of the complete system of the equations of motion, with consideration of continuous fluid stratification, nonlinear terms and terms responsible for turbulent exchange. It is found that a quasi-stationary vertical circulation cell is formed on the shelf under the influence of wind forcing, which favors upwelling. The cell is characterized by a coastal upwelling and lowering of waters in the area of sharp depth increase. Quasi-inertial reciprocal horizontal oscillations (with periods from 17 to 24 h) are generated in the open sea, and slowly decay after the termination of the wind action.

The water dynamics in the shelf zone off the Southern Coast of Crimea (SCC) are defined by the wind regime, then configuration of the coastline and the features of the bottom topography. Coastal upwelling can play an important role in the formation of the dynamic regime on the shelf of the SCC [1]. This phenomenon, observed near the Crimean coast, is a deep sea response to the wind forcing; it is encountered in narrow coastal regions where the transversal motion scale of motions is comparable with the baroclinic Rossby deformation radius.

Field measurements were carried out to study the physical processes in the upwelling zones, as for example, in the well-known experiments in the coastal waters of Oregon State, in the United States [11, 13] and in the northwestern part of Africa [16]. It should be noted that this phenomenon has not yet been studied completely. Thus, the obtained observations data give a basis for different hypotheses and ideas, suggested for the analytical and numerical models.

Paper [13] is one of the most interesting and fundamental works in this area. Besides the analysis of experimental data of the coastal upwelling on the Oregon shelf, obtained during two summer seasons, a model is suggested for the study of transfrontal circulation, which qualitatively describes the field data well. The authors used a stationary model, because the dominant time scale of the coastal upwelling is seasonal and consequently is much greater than the inertial one. Besides that, hydrostatic and geostrophic equilibrium was assumed along the coast. The vertical displacements and momentum diffusion were considered to be the most significant. Such integral approaches were developed in papers [2, 11, 14, 16].

The approximations used traditionally are not valid for the study of upwelling in the Black Sea. This is associated, for example, with the fact that the duration of wind forcing that causes upwelling near the SCC is hardly greater than one day, and thus the time scale of motion is comparable with the inertial one. The sharp depth increase in the region of the SCC does not allow us to stay within the hydrostatic approach for the scales named above.

All the points set forth above lead us to reject the assumption of the stationarity of the process, as well as the hydrostatic and geostrophic approximations during the formation of the problem of modeling the upwelling near the SCC. Besides, if we take into account the nonlinearity, the continuous stratification of the fluid, and the impulse character of the wind forcing (1–2 days), the consideration of these factors may lead to generation of such motions as were not found in other models of the coastal upwelling, in which different approximations were used.

The analysis of observational data during the upwelling near the SCC, which have not been adequately explained, indicates that as many factors as possible should be taken into account. One of these factors is the presence of near inertial spectral peaks, measured near the SCC [3].

The measurements of currents taken by clusters of synchronously working automatic moorings in the Black Sea in the study area near the SCC [5, 8] were used to obtain the characteristics of baroclinic gravity waves. One-dimensional spectra were plotted on the basis of measurements at different levels. Energy maxima of oscillations with periods of 21 and 23–25 h are clearly seen on these spectra, while peaks corresponding to the inertial period (17 h) are absent. The spectra, however, were not identified in any way, because they were one-dimensional. Thus, this result is cited here only as a fact registered during the experimental observations near the SCC.

Let us use a righthand coordinate system with the z-axis directed upwards. The plane $z = 0$ is located on the sea surface. We assume that the topography and environmental parameters are constant along the y-axis. It is shown in [7] that this assumption is valid for the study of coastal upwelling for time scales of up to 5–10 days, which is the scale of shelf waves. The stratification at the initial moment was taken from observational data. The Brunt–Väisäla frequency profile in the SCC region in summer is characterized, as a rule, by a well-expressed pycnocline at depths between 10 and 20 m with characteristic values of $(2–4) \times 10^{-2}$ s^{-1} at the buoyancy frequency peak. The bottom topography profile corresponded to the region between Simeiz and Yalta. The width of the area of variable depth changes here from 35 to 50 km. The sea depth on the shelf in the model calculations was limited by the 20-m isobath.

The system of equations that describes the dynamics of a continuously stratified fluid on an f-plane is reduced to the following system with respect to the stream function and vorticity:

$$\begin{aligned} &\Omega_t + J(\Omega, \Psi) - fV_z = g\rho_x/\rho_a \\ &\quad + k\Omega_{xx} + K\Omega_{zz} + (K\Psi_{zz})_z + K_z\Omega_z, \\ &V_t + J(V, \Psi) + f\Psi_z = kV_{xx} + (KV_z)_z, \\ &\rho_t + J(\rho, \Psi) + \rho_a g^{-1}N^2(z)\Psi_x \\ &\quad = r\rho_{xx} + (R\rho_z)_z + (R\rho_{0z})_z. \end{aligned} \tag{1}$$

Here, Ψ is the stream function ($\Psi_z = U, \Psi_x = -W$), $\Omega = \Psi_{xx} + \Psi_{zz}$ is vorticity; (U, V, W) is the velocity vector; ρ are the wave-induced density perturbations; ρ_a is the mean density; f is the Coriolis parameter; $k, r, K(z), R(z)$ are the coefficients of eddy viscosity and density diffusivity; J is the Jacobian; and $N^2(z)$ is the nondisturbed Brunt–Väisäla frequency profile.

Let us consider only the baroclinic response of the sea to wind forcing, thus we take the "rigid lid" condition and dynamic boundary conditions.

$$\Psi_x = 0, \quad KU_z = -\tau_x\rho_0^{-1}, \quad KV_z = -\tau_y\rho_0^{-1} \tag{2}$$

at the surface $z = 0$.

We take the kinematic nonslip conditions

$$\Psi_z = \Psi_x = V = 0 \tag{3}$$

at the bottom $z = H(x)$.

The tangential stresses τ_x and τ_y, caused by the wind field on the free surface, and which are part of boundary conditions (2) were calculated with the formulas: $\tau_x = \tau\cos\alpha$, $\tau_y = \tau\sin\alpha$, where τ is given by the expression $\tau = \rho_b C v^2$. Here, v is the wind speed, ρ_b is the air density, C is an empirical coefficient ($C = 1.6 \times 10^{-3}$ at $v \le 7$ m/s, $C = 2.5 \times 10^{-3}$ at $v \ge 10$ m/s), and α is the wind direction. The vertical profile $K_z(z)$ was chosen in accordance with the results of [6], and the coefficients of the horizontal eddy viscosity were taken from the interval between 10^1–10^2 m^2/s. The values of R, r were less by one order.

The following boundary conditions were used at the lateral boundaries:

$$\begin{aligned} &\text{at the coast} \quad \Psi_x = 0, \quad V = 0, \quad \rho = 0, \\ &\text{at the open boundary} \quad V_x = 0, \quad \rho = 0, \quad \Psi_x = 0. \end{aligned} \tag{4}$$

Problem (1)–(4) was solved numerically. The numerical scheme is discussed in detail in [4]. We note that before the construction of the numerical scheme, system (1) was transformed by substitution of variables connected with the bottom topography and stratification. Such substitution produces grid condensation in the layers with high vertical gradients and transforms the irregular region of calculation into a regular one.

Now we address the analysis of the numerical calculations. The situation typical for the SCC region in summer was modeled, when the wind forcing was of short duration (less than two days). The development of the coastal upwelling (downwelling) was studied as a result of the influence of the tangential wind stress on the free surface and the further decay of the motions after the wind forcing ceased.

The wind parameters (direction, speed) that cause upwelling (downwelling) in the studied area were taken from [9], where the results of observations of the wind field over many years over the Black Sea basin are presented (mean values of the wind speed, direction, recurrence). The northeasterly direction (along the coast) was chosen as the basic one, since it forms one of the typical situations when upwelling is generated. The meteorological scenario was modeled for a gradual increase in wind speed over an hour from 0 to 15 m/s. During the following 22 h, the wind speed and direction were constant and later, at the end of the day, the wind gradually decreased back to zero.

Let us consider the evolution of the model hydrophysical fields in the SCC region under the wind field parameters described above. The evolution of the motion, starting from the state of rest, can be divided into several stages: development, transition process, quasi-stationary state and decay. The first stage is the development while the wind is blowing, which lasts until $t = T$ (T is the time scale equal to 24 h). At the start (up to $t = 0.4T$), the longshore wind current is generated. It involves the upper 30-m layer and reaches velocities of 60 cm/s at the surface. The Coriolis force leads to the Eckman drift transverse to the coast, which is generated simultaneously with the longshore motion.

The Eckman motion is characterized by offshore motion in the upper layer, 30- to 40-m deep. The maximum velocities at the free surface in the direction perpendicular to the coast have the same values as the longshore ones. The water transport from the deeper

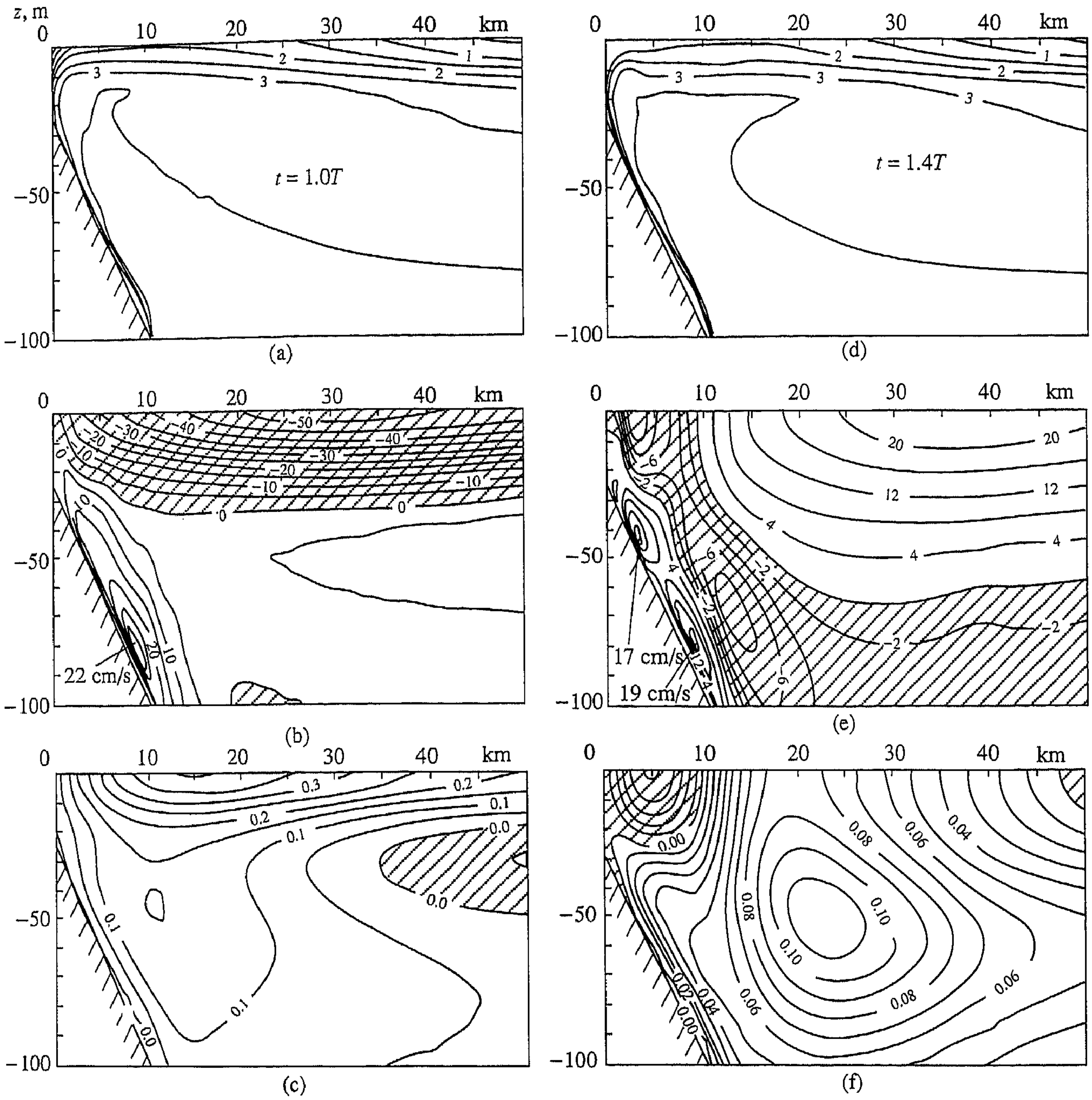

Fig. 1. (a, d, g, j) Isopycnic surfaces $\sigma_t(z)$–$\sigma_t(0)$ (kg/m^3), (b, e, h, k) components of velocity U (cm/s) and (c, f, i, l) V (m/s) at different moments t.

layers of the open sea to the shelf is induced in the deep layers (below the seasonal thermocline) due to the property of water continuity. The upward water motion on the shelf leads to the displacement of the pycnocline to the surface and its exposure at the surface in the shelf zone. The characteristic values of the vertical velocity of the fluid in the ascending water flows reach 1 mm/s.

After $t = 0.4T$, a subsurface longshore compensational countercurrent is generated in the open part of the sea at depths between 20 and 50 m, directed opposite to the wind. The characteristic values of the velocity in this current do not exceed 10 cm/s. The fields of the density and velocity components (U and V) at consecutive moments of time are presented in Fig. 1. The areas of negative values of the properties are dashed.

The situation that has developed by the time $t = T$ when the wind ceases is shown in Figs. 1a–1c. It can be seen that a day after the beginning of the wind forcing, the core of the pycnocline (isopycnal 2) rises to the surface.

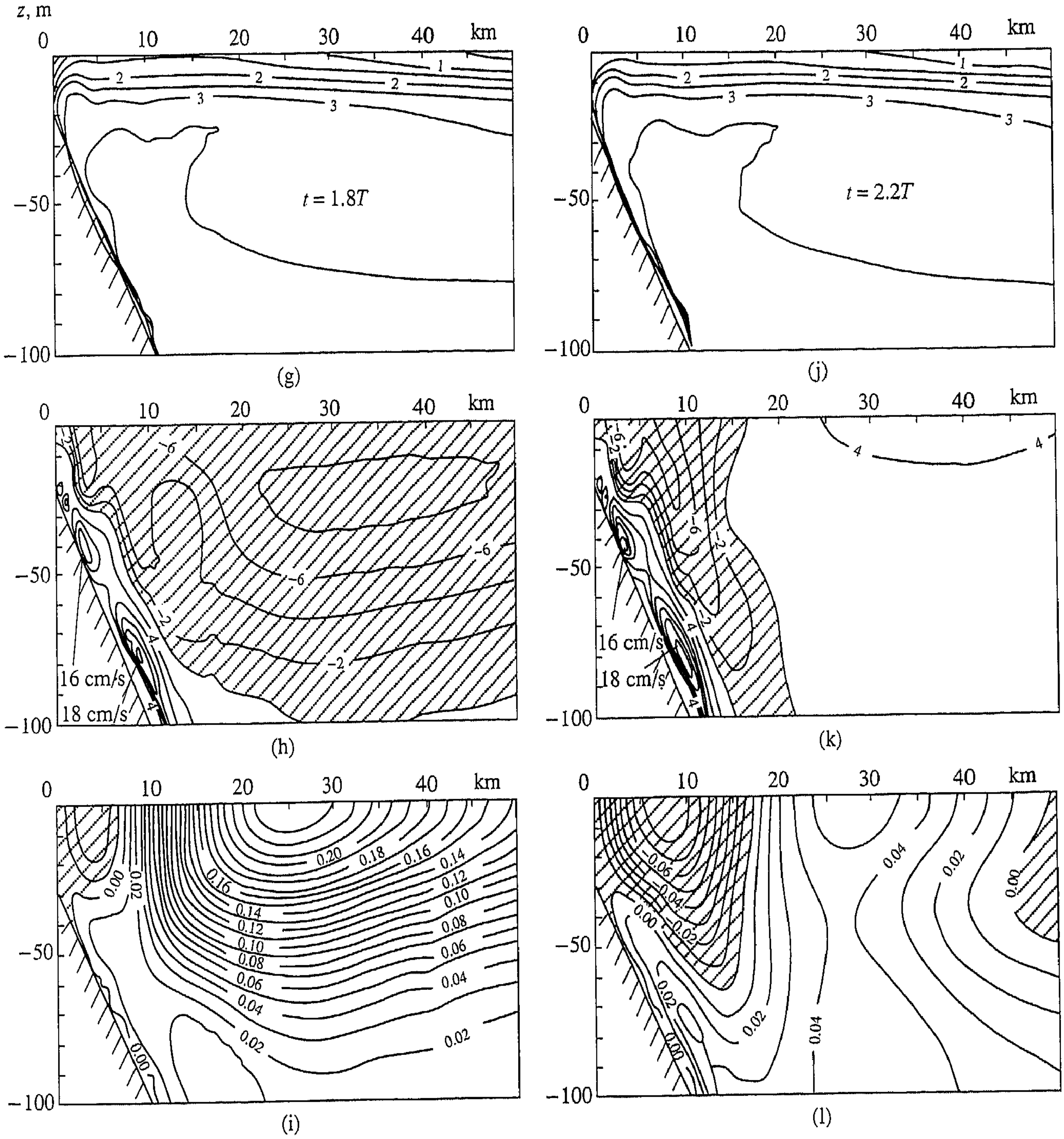

Fig. 1. (Contd.)

A frontal zone is formed in the shelf zone. The density gradient in the transversal direction to the coast reaches 0.5×10^{-4} kg/m^4.

The complicated pattern of the velocity fields U and V corresponds to the dynamic surface deformations which had occurred by the end of the day. By that time, the longshore velocity has a maximum at the free surface equal to 41 cm/s. It is located at a distance of ~15 km from the coast (Fig. 1c). There is a longshore countercurrent at a distance greater than 50 km from the coast at a depth of 30 m. The horizontal velocity here does not exceed 7 cm/s.

The velocities in the direction perpendicular to the coast have two extrema. The greatest values of the velocity in the coastward direction are observed in the nearbottom layers on the shelf 7–10 km away from the coast, and they reach 22 cm/s. The maximum velocities in the seaward direction are inherent to the water layers at the free surface 30 km from the coast, and they reach ~52 cm/s.

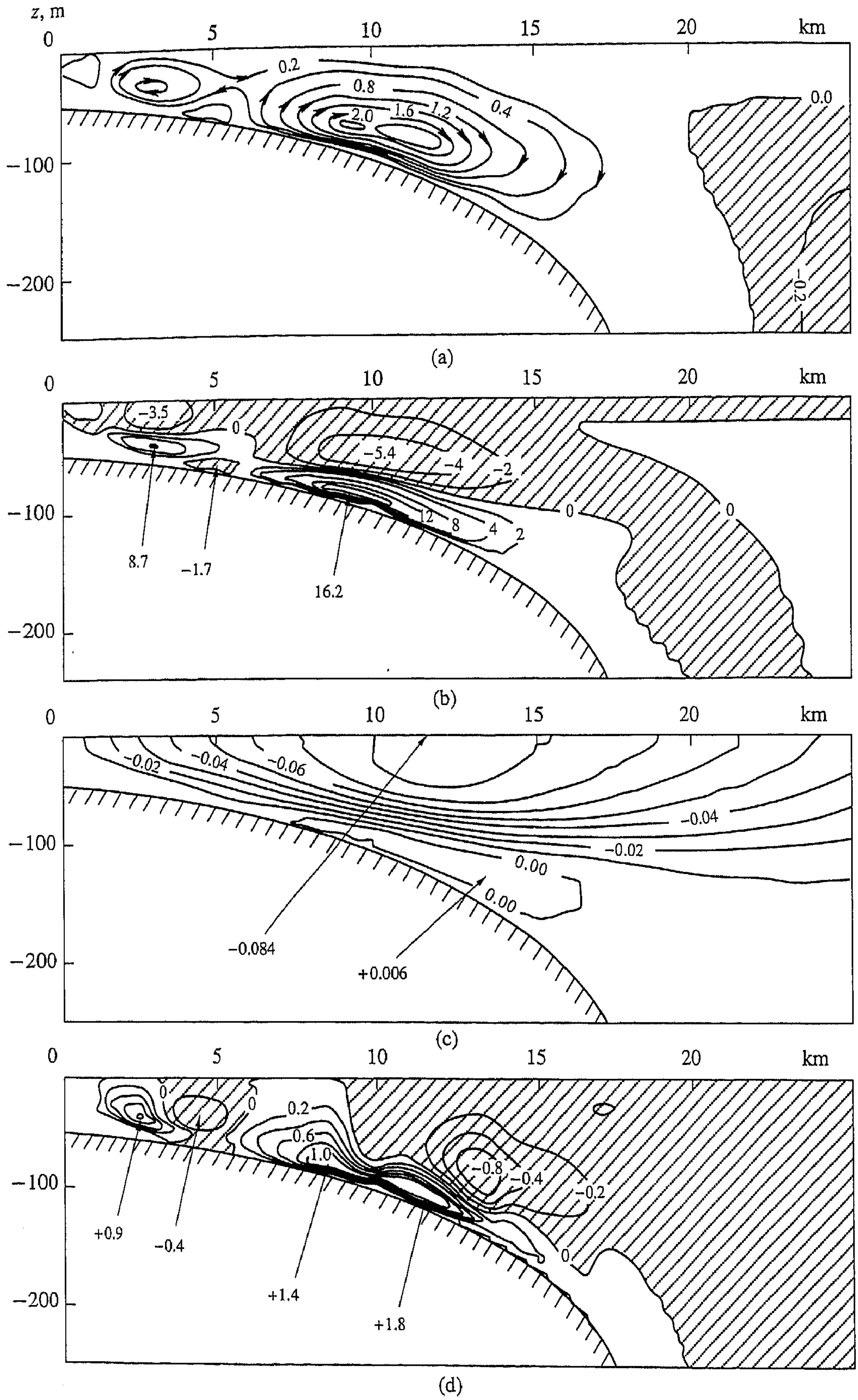

Fig. 2. (a) Stream function Ψ (m^2/s), (b) components of velocity U (cm/s), (c) V (m/s), and (d) W (mm/s) on the shelf at time moment $t = 3T$.

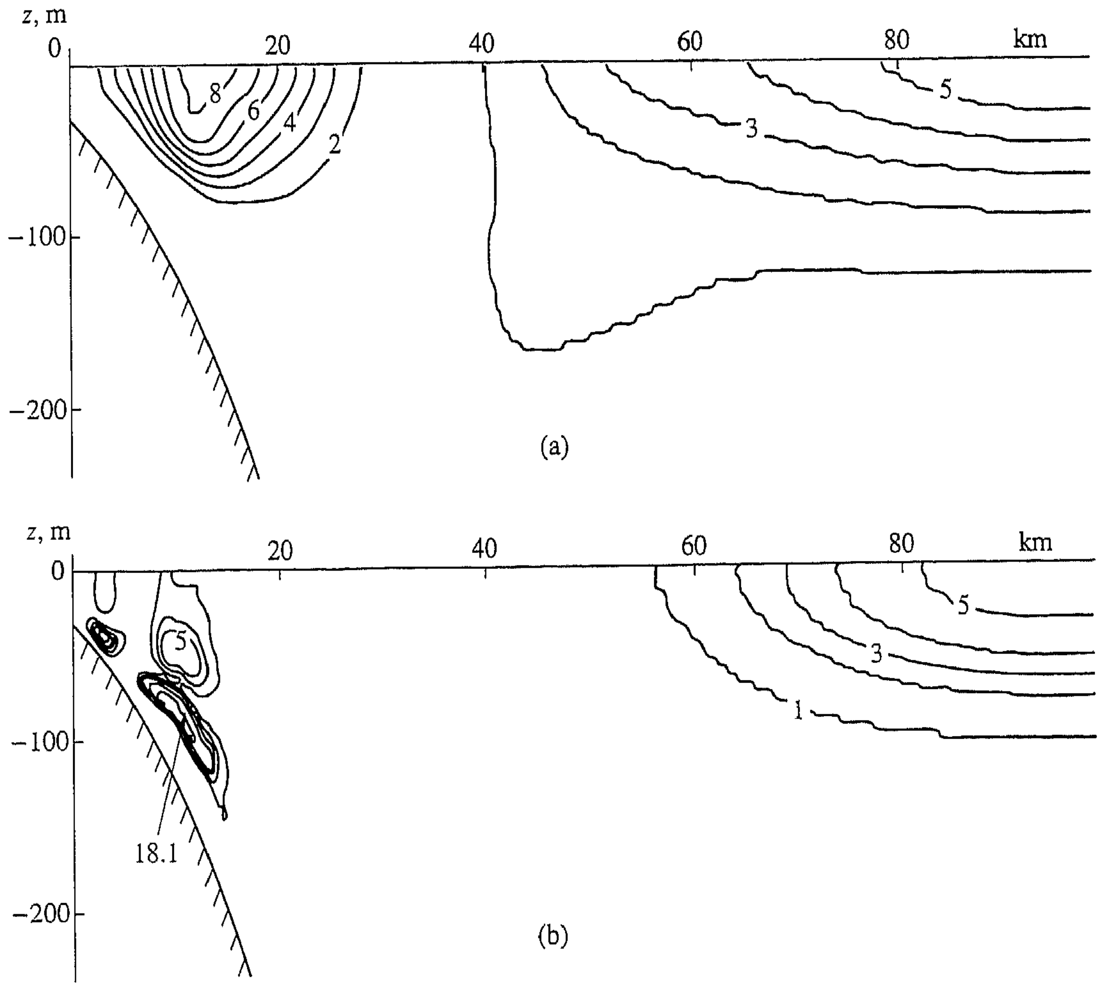

Fig. 3. Amplitudes of (a) the longshore V (cm/s) and (b) the coastward U (cm/s) velocity components.

The unbalanced dynamic system tends to return to a steady state after the termination of the wind forcing. Such a process is shown in Figs. 1d–1l. A comparative analysis of Figs. 1a, 1d, 1g, and 1j shows that after the external effect ceases, the density field tends to return to the initial state. The pycnocline lowers with time, and by the moment $t = 2.2T$, its axis is located between 10 and 12 m. There is no further lowering of the pycnocline to its initial undisturbed position, however. This lowering is prevented by the horizontal and vertical motions of the fluid particles that are formed on the shelf and maintain the horizontal density gradients. Let us analyze the structure that was formed in more details and study its temporal evolution.

A comparative analysis of Figs. 1b, 1e, 1h, and 1k shows that the velocity field U in the direction transversal to the coast can be divided conventionally into two areas. A vertical quasi-stationary advective cell is formed near the coast on the shelf (at a distance not greater than 20 km from the coast) as a result of wind forcing. This cell is characterized by a coastward flow near the bottom and a seaward flow in the upper layers (the values of the velocities are shown in Fig. 1). The parameters of this cell slightly change with time, but qualitatively, its shape is conserved. A quasi-stationary structure near the coast is also present in the field of the longshore velocity V (Figs. 1c, 1f, 1i, and 1l). High horizontal density gradients in the frontal zone, perpendicular to the coast, are maintained by the stationary geostrophic currents both along the coast and perpendicular to it. Let us analyze Fig. 2 for a more detailed analysis of the quasi-stationary motion in the nearcoast shelf zone, where the fields of the stream function and velocities U, V, and W are plotted for the moment $t = 3T$.

The analysis of Fig. 2 shows that the vertical advective cell has two cores, with their centers located at distances of 3 and 12 km from the coast. The horizontal scale of the cell (~17 km) corresponds to the first baroclinic Rossby deformation radius. The vertical motions are maximum near the bottom (Fig. 2d) and reach 2 mm/s. The structure of the isolines of the fields Ψ, U, and W clearly shows the vertical circulation on the shelf. It is characterized by the outflow of the bottom waters to the surface near the coast, accompanied by their sinking in the region of the sharp depth increase (Figs. 2a, 2d). The horizontal velocities (Fig. 2b) are maximum over and below the core of the cell, near the bottom and near the surface.

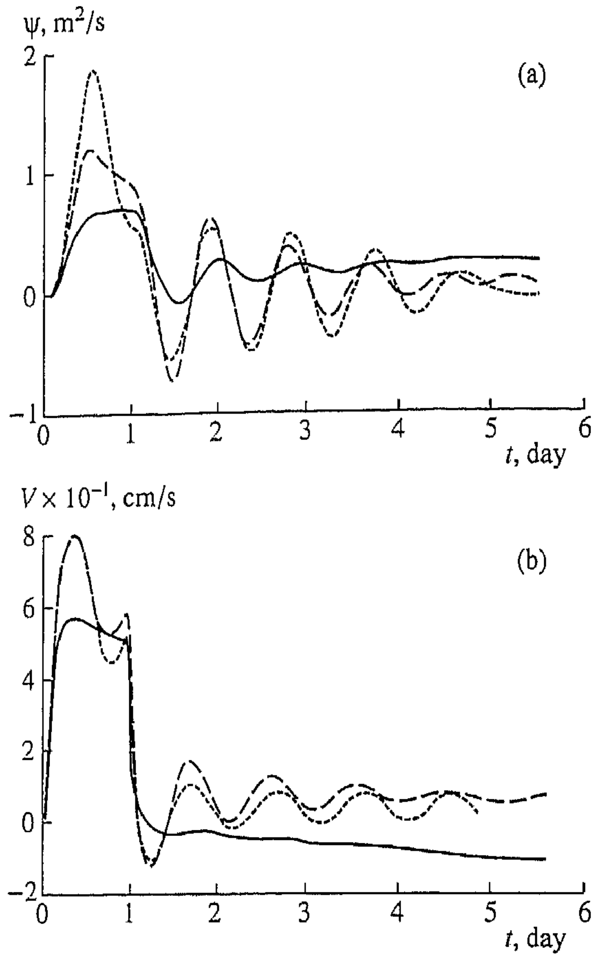

Fig. 4. Time dependences of (a) the stream function Ψ (m^2/s) at the 10 m level and (b) of the horizontal surface velocity $V \times 10^{-1}$ (cm/s) at different distances from the coast; the solid line refers to the shelf; the dashed line refers to the sharp depth increase; the dotted line refers to the edge of the continental slope.

The longshore velocity V (Fig. 2c) has a maximum at the free surface in the region of the advective cell core and is directed opposite to the wind. The velocity here reaches 8.4 cm/s. There is a weak jet countercurrent in the same direction as the wind. The velocities here, however, do not exceed 1 cm/s.

The field of the longshore velocity V (Figs. 1c, 1f, 1i, and 1l) is also variable. It gradually changes in time with oscillating motions. Unlike the velocity U, the oscillations here occur not with respect to the zero state but against the background of the stationary longshore current directed in accordance with the wind. The oscillations of the velocity V in different parts of the section (x, z) have different amplitudes. The maximum amplitude of the oscillations within the time interval $(1–2)T$ is equal to 25 cm/s and is concentrated on the free surface at a distance of ~30 km from the coast. The oscillations decay with time.

Let us analyze the spatial characteristics of the field of the stationary longshore velocity V and address Fig. 3a for this purpose, where the amplitude field calculated during the time interval $t = (2–3)T$ is shown. It can be seen that besides the motions trapped by the bottom topography near the coast that were considered earlier (Fig. 2), there is an area of intensive motions in the open part of the sea. The maximum velocities V are concentrated here in the upper 100-m layer. The amplitude field of the velocities V, shown in Fig. 3a, is plotted, with consideration of both the stationary longshore current and the oscillatory motion. The field of the amplitudes of velocities U (Fig. 3c) corresponds to this field. Unlike the field of V, the velocity U in the distant zone is characterized only by oscillations near the zero level. The stationary advective cell near the coast that was described in details above (Fig. 2b) is also seen in Fig. 3c.

Let us address Fig. 4 to reveal the nature of the generated oscillations and study their characteristics. The time dependencies are shown here of the longshore velocity V and the stream function Ψ, which characterizes the velocities U and V at three points: on the shelf, over the sharp depth increase and on the border of the continental slope. The analysis of Fig. 4 shows that two types of motion can be distinguished in the area of the calculations. After the initial outburst of all of the three values during the wind forcing ($0 < t < T$), the velocities U and V reach a stationary condition after several decaying oscillations (the solid line in Fig. 4a). This stationary condition is defined by the presence of the vertical quasi-stationary cell described above. The velocity V also reaches a stationary regime on the shelf (the solid line in Fig. 4b).

Another type of motion is present in the region of the sharp depth increase and in the open sea. The stream function field is characterized here by decaying oscillations near the zero state (the dashed and dotted lines in Fig. 4a). These oscillations can be seen for a period of five days after the wind forcing ceases. The analysis of the periods of these oscillations shows that they are close to inertial ($T_{in} \approx 17$ hours). Besides, as can be seen from Fig. 4a, it is obvious that if the period of oscillations is different at different points, it can also change with time. This fact corresponds to the continuous evolution of motions in time and different hydrophysical conditions at various levels of fluid.

It is known [12] that the fluid stratification and its relative vorticity caused by the induced currents may lead to the shift of the frequencies of oscillations with respect to the inertial one. We obtained here, after analysis of the numerical calculations results, that the oscillation periods are close to inertial in the deep layers of the open sea. In the layers close to the surface, these values can increase up to 23–24 h. The oscillations of the velocity V occur with the same periods as for the velocity U, but they develop, however, against the background of the perturbed stationary current (the dashed and dotted lines in Fig. 4b).

Let us briefly summarise the conclusions. A short-term action of the longshore wind, which favors upwelling, leads to a seaward water flow in the upper layer to a depth of 30 m and to a coastward compensational flow in the nearbottom layers, accompanied by the rising of the isopycnals near the coast and the exposure of the pycnocline at the surface. A compensational longshore subsurface countercurrent is generated at the same time in the open sea in the depth interval from 20 to 70 m. The maximum values of the horizontal velocity directed away from the coast (for a wind speed of 15 m/s) are 60 cm/s at the surface and ~20 cm/s for the coastward currents near the bottom.

After the wind forcing ceases, the hydrodynamic system tends to return to the state of rest. The isopycnals tend to deepen to their initial position. The decay processes in different areas of the basin, however, are of different types. One day after the termination of the wind forcing and decay of the oscillations, a circulation cell is formed on the shelf, characterized by an outflow of bottom waters to the surface near the coast and a sinking of the surface waters to the bottom in the region of the shelf break. The characteristic vertical velocities in the circulation cell during the first stage were equal to ~0.5 mm/s. The horizontal size of the cell is about 15 km (equal to the baroclinic Rossby deformation radius).

The decay of the motion in the open sea has an oscillating character. Reciprocal horizontal oscillations with periods from inertial (~17 h) to one day are generated in the upper 100-m layer during the first stage of the upwelling. The period of oscillations is different at different points of the basin and can change with time. The oscillations slowly decay and may be traced one week after the termination of the wind forcing.

REFERENCES

1. Arkhipkin, V.S., Eremeev, V.N., and Ivanov, V.A., Upwelling in Ocean Boundary Regions, *Preprint of Marine Hydrophysical Inst., Ukr. Acad. Sci.*, Sevastopol, 1987.
2. Belousova, E.I., Numerical Modeling of Stationary Offshore and Onshore Currents in the Coastal Zone, *Morsk. Gidrofiz. Issled.*, 1982, pp. 54–62.
3. Blatov, A.S. and Ivanov, V.A., *Gidrologiya i gidrodinamika shel'fovoi zony Chernogo morya* (Hydrology and Hydrodynamics of the Black Sea Shelf Zone), Kiev: Naukova Dumka, 1992.
4. Vlasenko, V.I., A Nonlinear Model of Baroclinic Tides Generation over Long Inhomogeneities of the Bottom Topography, *Morsk. Gidrofiz. Zh.*, 1991, no. 6, pp. 9–16.
5. Ivanov, V.A. and Yankovskyii, A.E., *Dlinnovolnovye dvizheniya v Chernom more* (Long Wave Motions in the Black Sea), Kiev: Naukova Dumka, 1992.
6. Kolesnikov, A.G. and Boguslavskii, S.G., Vertical Transport in the Black Sea, *Morsk. Gidrofiz. Issled.*, 1978, pp. 33–47.
7. *Modelirovanie i prognoz verkhnikh sloev okeana* (Modeling and Forecast of the Upper Ocean Layers), Leningrad: Gidrometeoizdat, 1979.
8. *Nauchno-tekhnicheskii otchet o rabotakh v 14-m reise NIS "Professor Kolesnikov"* (Scientific–Technical Report on the Works on Cruise 14 of R/V *Professor Kolesnikov*), Available from Scientific Archives of Mar. Hydrophys. Inst., Ukr. Acad. Sci., 1986, Sevastopol, vol. 1, part 1.
9. *Tipovye polya vetra i volneniya Chernogo morya* (Typical Fields of Winds and Wind Waves of the Black Sea), Sevastopol: Sevastopol Otd. Gos. Okeanogr. Inst., 1987.
10. Csandy, G.T., *Circulation in the Coastal Ocean*, D. Reidel, 1982.
11. Hayes, S.P. and Halpern, D., Observations of Internal Waves and Coastal Upwelling of Oregon Coast, *J. Mar. Res.*, 1976, vol. 34, pp. 247–267.
12. Kunze, E., Near-Inertial Wave Propagation in Geostrophic Shear, *J. Phys. Oceanogr.*, 1985, vol. 15, no. 5, pp. 544–565.
13. Mooers, C.N.K., Collins, C.A., and Smith, R.L., The Dynamic Structure of the Frontal Zone in the Coastal Upwelling Region off Oregon, *J. Phys. Oceanogr.*, 1976, vol. 6, pp. 3–21.
14. Ou, H.W., Wind-Driven Motion Near a Shelf-Slope Front, *J. Phys. Oceanogr.*, 1984, no. 14, pp. 985–993.
15. Thompson, J.D. and O'Brien, J.J., Time-Dependent Coastal Upwelling, *J. Phys. Oceanogr.*, 1973, vol. 3, no. 1, pp. 33–46.
16. Tomczak, M., Jr., Continuous Measurement of Near Surface Temperature and Salinity in the NW African Upwelling Region between Canary Island and Cap Vert during the Winter of 1971–1972, *Deep-Sea Res.*, 1977, vol. 24, no. 12, pp. 1103–1119.